Original Paper _____ *Forma*, **19**, 13–23, 2004

Neural Coding of Color

Naoya YOKOYAMA, Koichi SHODA and Yoshi TAMORI*

Human Information System Laboratory, Kanazawa Institute of Technology,
3-1 Yakkaho, Matto, Ishikawa 924-0838, Japan
**E-mail address: yo@his.kanazawa-it.ac.jp*

(Received February 1, 2004; Accepted March 15, 2004)

Keywords: Topological Mapping, Spatiotemporal Representation, ICA

Abstract. We measured multi-channel MEG (MagnetoEncephaloGraphy) responses to a set of color stimuli (for twelve colors). Subjects are gazing at colored squares during the measurements. Each ECD (Estimated Current Dipole) in the brain, thus localized response to the corresponding color stimulus, is moving inside area V4α (BARTELS and ZEKI, 2000), showing a characteristic orbital path. In our measurements, absolute positional-errors are still large. However, the relative resolution is quite high, since the orbits of ECDs are localized in quite a small volume (1 [cm^3]). This localized volume corresponds to V4α. ECDs in the volume are forming different orbits from each other. V4α conserves topological relation in the chromatic coordinate. Our results suggest that the neural coding of chromaticity topologically corresponds to well known geometrical coding of chromaticity in terms of a continual deformation between neighboring representations. Therefore, the observations could be interpreted as that the chromatic topology is represented in V4α and that the refined coding of each color is spatiotemporally represented within V4α. This fine spatiotemporal resolution in the results is obtained by our non-parametric gICA (geometric Independent Component Analysis) algorithm based on the isotropy condition of connections among adjacent tangential spaces in the neural activities.

1. Introduction

We all have almost complete understanding for the coding in color system by means of a long-term accumulation of intensive research. A color is represented by a vectorial quantity. Color system is depicted in an elegant three-dimensional coordinate system. Using the color system, we can quantitatively observe/represent/specify a color. In spite of this successful pursuit, we have never been able to obtain the knowledge how the color perception is coded in the brain, thus the neural coding of color perception. We measured multi-channel MEG responses to a set of color stimuli (for twelve colors). Generally, an error in the absolute position of the local activity, which is calculated as a solution to the inverse problem, could be large in a MEG measurement. However, the relative positions from one another provide quite detail information of the responses. We investigate the

coding of color and the color system, by observing refined MEG responses, based on non-parametric gICA.

It is well known that the primary perceptional space is mapping to the cortical area in a topology-preserving manner. For example, neighboring neurons' signals in the primary visual cortex code similar inputs that are neighboring positions in the visual field. However, the topology of color space (e.g. CIE chromaticity space) is not known to be conserved in V4. All the color stimuli activate V4/V4α, though V4 has a retinotopy (BARTELS and ZEKI, 2000).

2. Methods

We measured detail MEG responses to color stimuli. In order to find a set of isoluminant color stimuli, we first carried out heterochromatic flicker photometry in experiment 1. Then, MEG responses were measured during color presentation tasks, using whole head type 160ch MEG system in KIT. In the MEG measurements, we investigated so-call "retinotopy" within V4/V8 region in experiment 2. In experiment 3, we tried to elucidate how the topology in a chromatic space could be represented in V4α, using the detail analysis of MEG data. Subjects were 5 right-handed healthy males. ECDs responding to the presented set of stimuli are estimated by solving the inverse problem for all the MEG data that were preprocessed by non-parametric gICA algorithm.

2.1. Experiment 1—hetero-chromatic flicker photometry

Physiological evidence suggests that colors and luminance are represented separately in the primate visual system (e.g. LIVINGSTONE and HUBEL, 1988.) A major pathway of the luminance channel is through the magnocellular pathways. This is the pathway that goes

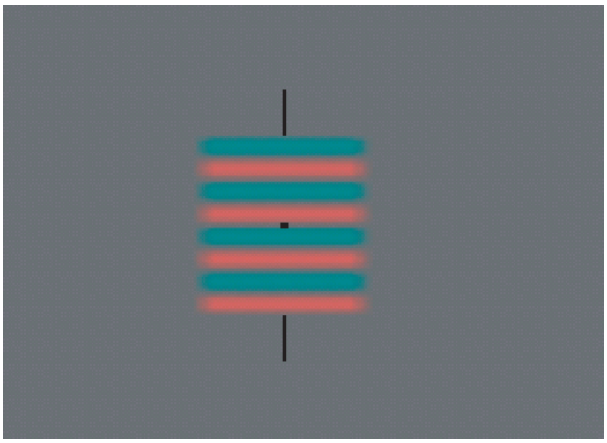

Fig. 1. Stimulus for experiment 1: The size of grating stimuli is 1.5×1.5 [deg^2]. There are 8 alternating opponent colored lines in the grating. These lines are moving upward with the speed of 1.42 [deg/sec]. The averaged luminance of the stimuli was controlled so as to be 9.742 [cd/m^2].

through the magnocellular layers of the lateral geniculate nucleus. On the other hand, the chromatic pathway is through the parvocellular layers of LGN.

These two aspects of visual stimuli could activate multiple positions in the brain simultaneously.

Such activities possibly form multiple current dipoles simultaneously. The estimation algorithm fails to estimate the positions of such multiple dipoles in time. Especially, a luminance change induces large MEG responses. Therefore, we have to minimize the possibility that the luminance change may affect chromatic responses. For that purpose, we calibrated the luminance of all twelve colors to a sensation-equated one by heterochromatic flicker photometry (Fig. 1) (KELLY and VAN NORREN, 1977). We used color-grating stimuli for the experiment. There are 8 alternating opponent colored lines in the sinusoidal grating. These lines are moving upward with the speed of 1.42 [deg/sec]. The averaged luminance of the stimuli was controlled so as to be 9.742 [cd/m^2]. This luminance was also chosen for the gray background. The pairs of opponent colors were chosen from the opponent colors on three color-confusion lines

$$y = -0.1942x + 0.3981$$

$$y = -0.55357x + 0.517857$$

$$y = 2.0534x + 0.35113$$

for this experiment.

2.2. Experiment 2—retinotopy in V4

According to preceding researches, V4 has a kind of retinotopy. They shows that color stimuli in upper visual field are represented medially in V4 (MCKEEFRY and ZEKI, 1997)

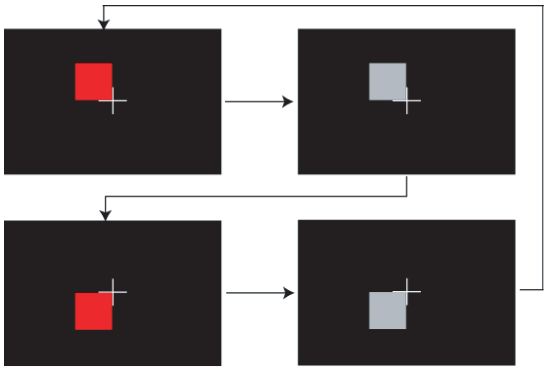

Fig. 2. A snapshot of a stimulus sequence for experiment 2: Pair of chromatic and monochromatic stimuli were alternately presented in lower or upper visual field. Each stimulus was presented during 600 [m sec] for color images, 300 [m sec] for monochromatic images.

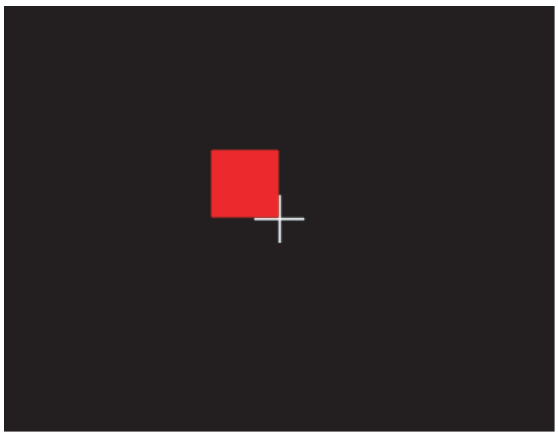

Fig. 3. A snapshot of a stimulus sequence for color presentation tasks (experiment 3): Subjects were gazing the fixation point (white cross). At the center in the left-upper quarter, a colored square is shown in the figure as an example. Chosen colors for the stimuli are shown in Fig. 4.

or V8 (HADJIKHANI *et al.*, 1998) and color stimuli in lower visual field are represented laterally in V4/V8. In order to confirm the existence of a retinotopic mapping in V4/V8, we presented color stimuli in both the upper field and the lower field alternately to the subjects, Fig. 2.

2.3. Experiment 3—topological analysis

Twelve color stimuli (1.5 [deg] × 1.5 [deg] square) were presented at the center in the left-upper quarter (Fig. 3). In order to prevent from that areas responding to each quarter around the fixation point are widely spreaded in the brain, the decentered stimuli were chosen. The colors of stimuli were chosen from the topologically circular path on the CIE *xy* chromaticity diagram (Fig. 4). These colors along the chromatic circle were presented sequentially and/or randomly, while each presentation lasts 300 [m/sec].

3. Analysis

160ch data were treated by non-parametric gICA (geometric Independent Component Analysis) in both the time and frequency domain. Only a few independent components were obtained within the visual cortex. Our non-parametric gICA algorithm is explained in the next section. The independent components were combined into a temporal component. Estimated current dipoles (ECDs) were plotted with MRI sections. Basically, the absolute position of ECD could have an error ranging within $2 \times 2 \times 2$ [cm^3] volume. This is because the large error comes from superimposition procedure of ECD on MRI image. On the other hand, if the dipoles are ideally single ones, the relative error in the positions of ECDs is less than 1 [mm^3] volume size in our MEG apparatus. The positional estimation of single dipole is not so-called ill-posed problem. If we could successfully separate the raw data into

independent components from one another, each component is considered to be an ideally single dipole. Therefore, we, in the first place, carry out gICA calculations with the experimental data so that we can obtain independent components of the data. Then we can calculate the ECD from each independent component of MEG responses.

3.1. Non-parametric gICA

Consider N independent activities $(s^1(t), ..., s^N(t))$ in the brain. We cannot directly measure the activities, but we can observe L instantaneous mixtures $(x^\nu(t), \nu = 1, ..., L)$ of the modulated magnetic fields of the activities via L SQUID (Superconducting QUantum Interference Device) sensors. The observed signals $(x^1, ..., x^L)$ are written by

$$x^\nu(t) = A_j^\nu s^j(t), \tag{1}$$

where $A_j{}^\nu$ is $L \times N$ mixing matrix which does not depend on t. In formula (1) in which, following Einstein's convention, the summation sign has been suppressed, the index j take, successively and independently of one another, all the values $1, 2, ..., N$. In the present text, we identify the element $A_j{}^\nu$ with the matrix itself $\mathbf{A}$ and if one of the suffixes of the element notation $A_j{}^\nu$ is fixed by a value (e.g. $j = a$), we regard it as a vector $A_a{}^\nu$. It would be useful to adopt the convention in which Greek suffices such as μ, ν run from 1 to L and English suffices such as $i, j, k, ...$ run from 1 to N here after. If we can find a set of N vectors $\overline{w}_\nu^1$, $\overline{w}_\nu^2, ..., \overline{w}_\nu^N$ which satisfy

$$s^i(t) = \overline{w}_\nu^i x^\nu(t), \tag{2}$$

putting Eq. (2) into Eq. (1), we obtain

$$\overline{w}_\nu^i A_j^\nu = \delta_j^i = \begin{cases} 1 & i = j \\ 0 & i \neq j. \end{cases} \tag{3}$$

Therefore, the matrix $\overline{w}_\nu^i$ in the element notation of a set of N vectors $\overline{w}_\nu^1, \overline{w}_\nu^2, ..., \overline{w}_\nu^N$ should behave as an inverse matrix of $A_j{}^\nu$. We are interested in a set of independent source signals $(s^1(t), ..., s^N(t))$. Generally, $N \leq L$, since we consider a set of neural activities which represent a function within a localized area in the brain. Let us extend the dimension N to L. Later, the dummy independent vectors $\overline{w}_\nu^{N+1}, \overline{w}_\nu^{N+2}, ..., \overline{w}_\nu^L$ will be neglected. It requires for a set of vectors $\overline{w}^1, \overline{w}^2, ..., \overline{w}^L$ to form an independent base. Therefore, the independency among the vectors requires that the volume

$$V = \overline{w}_\nu^1 \wedge \overline{w}_\mu^2 \wedge \cdots \wedge \overline{w}_\lambda^L \tag{4}$$

should be maximized. Let us divide a component $s^j(t)$ into several monotonic parts ranging over (a_n, a_{n+1}) in nth part for example. The inverse function of the nth part $s_n^j(t)$,

$$\Delta t_n = \left[s_n^j \right]^{-1}(s) \quad s \in (a_n, a_{n+1}) \tag{5}$$

gives a lapse time Δt_n of the activity change in the domain (a_n, a_{n+1}). Accumulated time for each independent component is calculated by

$$T = \sum_n \int_{(a_n, a_{n+1})} \left[s_n^j \right]^{-1}(s) ds \tag{6}$$

which does not depend on j. Our goal is to find optimum set of weight vectors $\overline{w}_v^1$, $\overline{w}_v^2$, ..., $\overline{w}_v^N$ that satisfy Eq. (2). Let us put a set of tentative signals $y^1(t)$, ..., $y^N(t)$ which is written by

$$y^j(t) = w_v^j x^v(t) \tag{7}$$

where $w_v{}^1$, $w_v{}^2$, ..., $w_v{}^L$ is tentative set of weight vectors. Accumulated time for these tentative signals are written by

$$T^j = \sum_n \int_{(a_n, a_{n+1})} \left[y_n^j \right]^{-1}(y) dy \quad j = 1, ..., N. \tag{8}$$

Here, we assume an isotropy of external/global frame of reference. In order to implement the isotropy condition, let us minimize the volume of $(T^1, ..., T^N)$ under the condition that the weight vectors are independent of one another (maximizing V in Eq. (4)), defining the loss function

$$L(w) = -\ln\left(w_\alpha^1 \wedge w_\beta^2 \wedge \cdots \wedge w_\lambda^L \right) + \ln\left(\prod_{j=1}^N T^j \right). \tag{9}$$

To find the optimum weight matrix, we take the natural gradient (AMARI, 1998) learning as follows:

$$\tau \frac{dw_\mu^k}{dt} = -\frac{\partial L(w)_T}{\partial^T w_k^\lambda} w_\ell^\lambda w_\mu^\ell. \tag{10}$$

Using our loss function (9), the learning equations are given by

$$\tau \frac{dw_\mu^k}{dt} = \left(\delta_\ell^k - \frac{1}{T^k} \sum_n \left[y_n^k \right]^{-1} \left(y^k \right) y^\ell \right) w_\mu^\ell. \tag{11}$$

Putting

$$\varphi\left(y^k\right)=\frac{1}{T^k}\sum_n\left[y_n^k\right]^{-1}\left(y^k\right), \tag{12}$$

Eq. (11) leads to conventional ICA algorithm

$$\tau\frac{dw_\mu^k}{dt}=\left(\delta_\ell^k-\varphi\left(y^k\right)y^\ell\right)w_\mu^\ell \tag{13}$$

under the *natural gradient* condition, whereas the nonlinear function $\varphi(y)$ is determined/

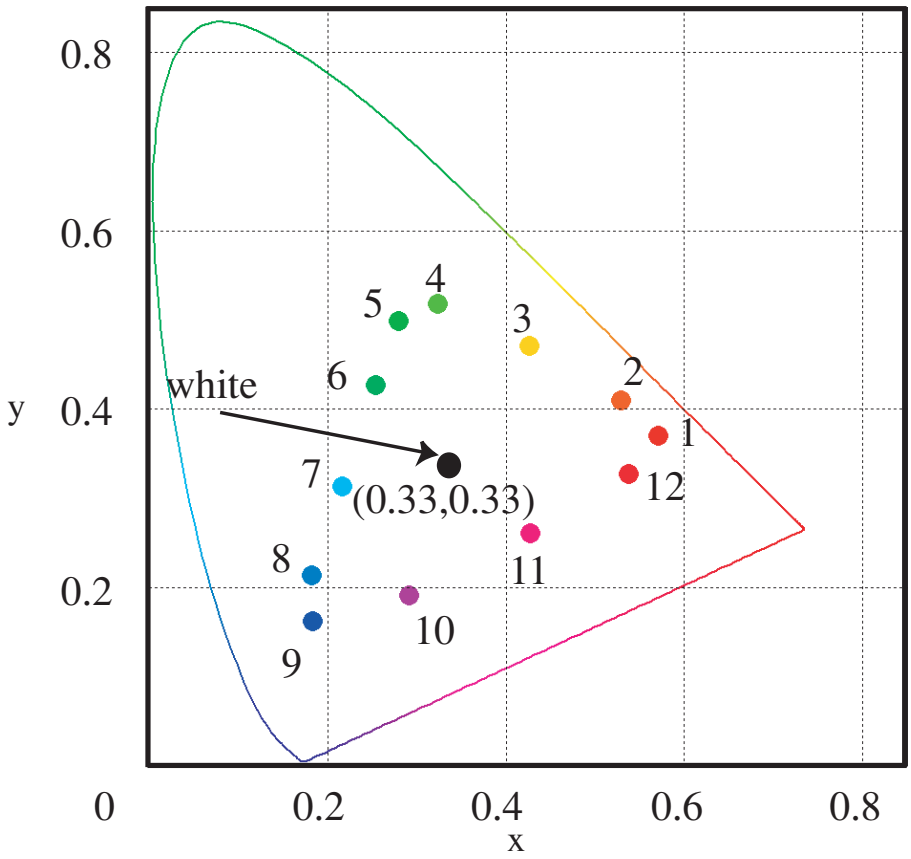

Fig. 4. Chosen colors for stimuli in experiment 3: Chosen colors for stimuli are plotted in CIE chromatic *xy*-coordinate. These twelve colors' luminances are calibrated so as to be sensation-equivalent with each other. Each color is numbered as shown in the figure.

recalculated by the numerical data with Eq. (12). In the equilibrium of Eq. (13), we can obtain the optimum weight vectors $\overline{w}_v^j$ and the independent components by Eq. (2). In spite of that the derivation of Eq. (11) is based on purely geometrical view in the signal space, we reach Eq. (13) which is the same formula as of conventional ICA. In our derivation, however, Eq. (12) has to be always recalculated. Therefore, we cannot assume the probability density function of y^k.

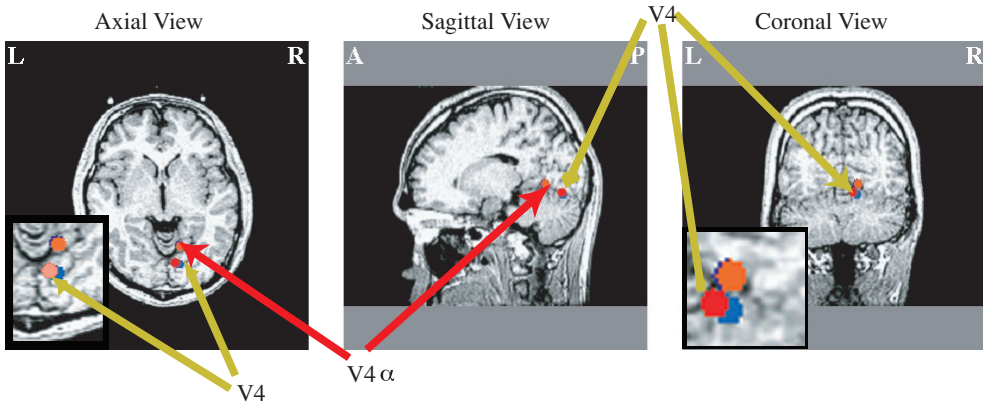

Fig. 5. ECDs corresponding V4/V4α: The blue dot represents lower visual field stimulation. The red dot represents upper visual field stimulation. The orange dot was activated by both upper and lower stimulations and there was no difference for those stimuli in different positions. The insets show the expanded images of V4/V4α, thus the medially anterior bank of fusiform gyrus. Colored version of this figure can be seen in the WEB of FORMA Journal Vol. 19, No. 1 with URL: http://www.scipress.org/journals/forma/frame/19.html

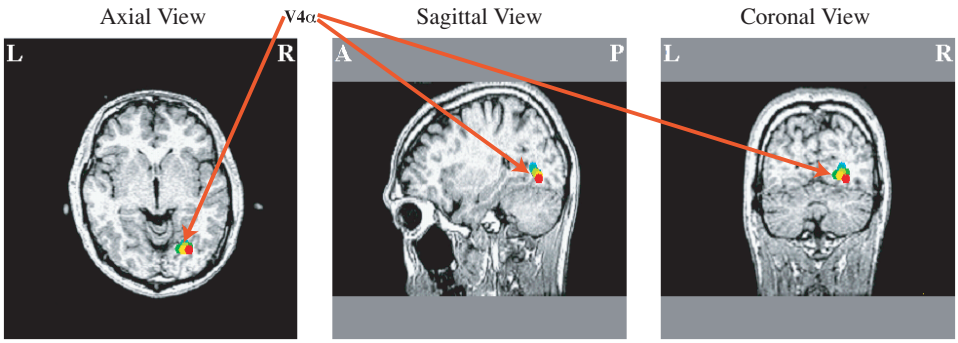

Fig. 6. The absolute positions of current dipoles estimated by combined independent components within V4α: ECDs are moving inside the small volume (1 [cm^3]) shown by colored dots. Colored version of this figure can be seen in the WEB of FORMA Journal Vol. 19, No. 1 with URL: http://www.scipress.org/journals/forma/frame/19.html

4. Results of Retinotopic Experiment (experiment 2)

Figure 5 shows ECD components observed in visual cortices in experiment 2. The blue dot represents lower visual field stimulation. The red dot represents upper visual field stimulation. This retinotopic representation is called V4 or V8. The size of the displacement between the ECDs in V4 was 4.1 [mm]. The orange dot was activated by both upper and lower stimulations and there was no difference for those stimuli in different retinotopic positions. It is reported that an anterior satellite that is called V4α has no retinotopy. Therefore, the anterior component is not showing retinotopy, whereas the posterior components show a weak retinotopy. The preceded study (McKeefry and Zeki, 1997; Bartels, 2000) is confirmed by the results of our apparatus.

5. Results of Topological Experiment (experiment 3)

Figure 6 shows the absolute position of current dipoles estimated by combined independent components within the visual cortex. The ECD is moving inside the 1 [cm^3] volume of medially anterior bank of fusiform gyrus. This position corresponds to V4α (Bartels, 2000). The intensity of this ECD increases around the latency of 100 msec after the onset of the stimulus. This activity was identified for all the participants in the present

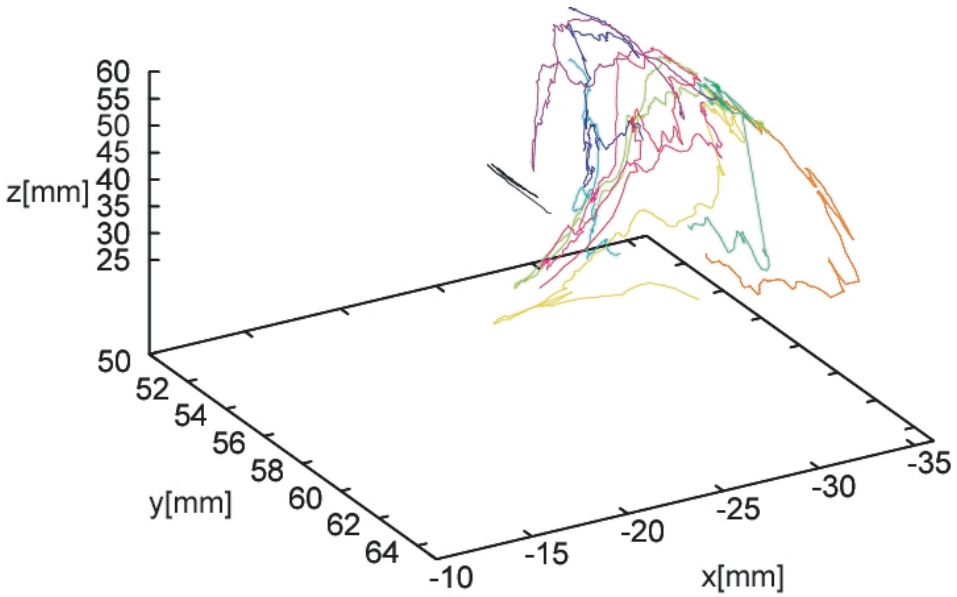

Fig. 7. Refined orbits of ECDs inside V4α: The small volume shown in Fig. 6 is expanded in this figure. ECDs that are responding to the presented twelve colors are all localized in V4α, though the shapes of them are different from each other. Colored version of this figure can be seen in the WEB of FORMA Journal Vol. 19, No. 1 with URL: http://www.scipress.org/journals/forma/frame/19.html

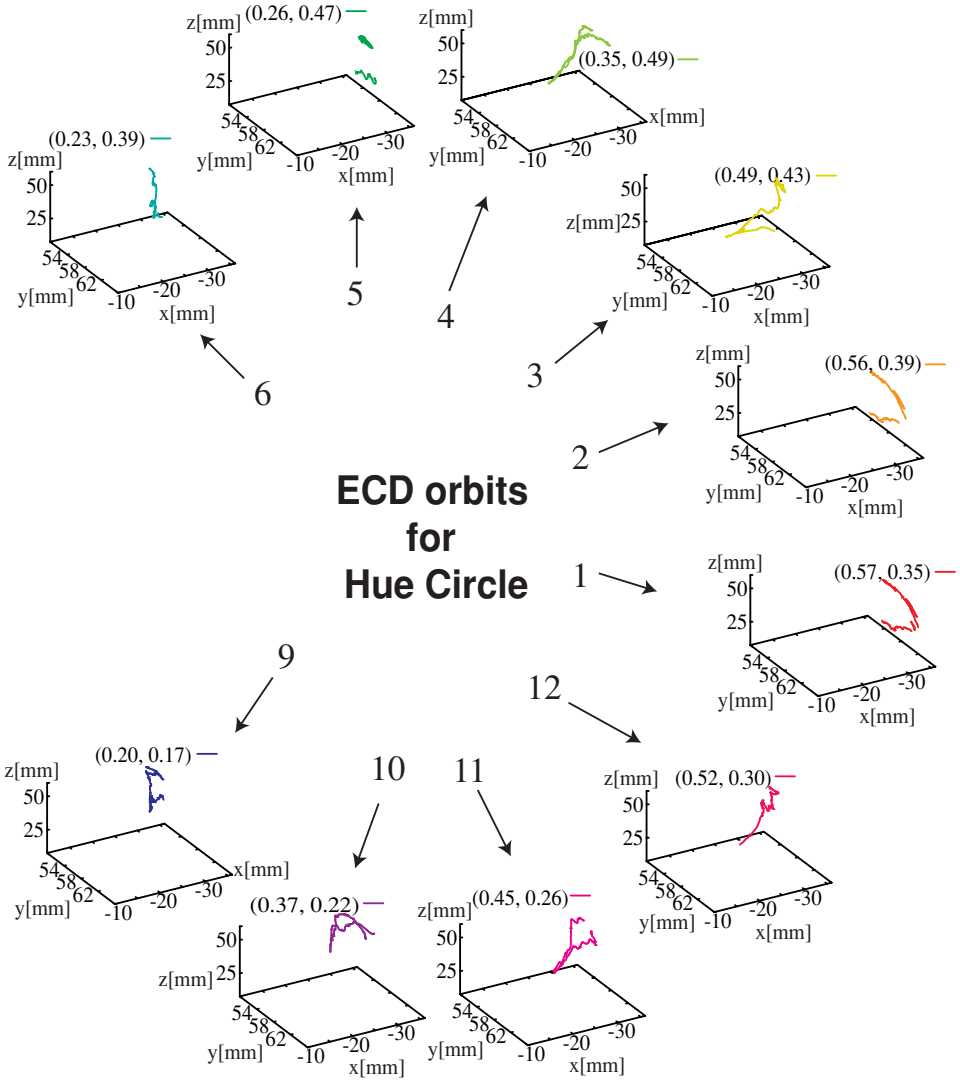

Fig. 8. The refined orbits for each color stimulus: The legend of each plot represents the *xy* values in CIE chromatic coordinate. The numbers pointing each curve correspond to the ones in Fig. 4. Colored version of this figure can be seen in the WEB of FORMA Journal Vol. 19, No. 1 with URL: http://www.scipress.org/journals/forma/frame/19.html

study. The spatial segregation in neural representations of upper and lower field, thus the retinotopy, was not observed in this area. Figure 7 shows the refined orbits of ECDs corresponding to twelve colors were overlapped in the MRI coordinate. The overall orbit forms a 2-dimensional surface that corresponds to the anterior bank of fusiform gyrus. The size of the overall area covered by the orbits was approximately 1.5 [cm^2]. The gray line

in Fig. 7 represents the orbit of the ECD that is responding to the luminance change in the control experiment. This luminance-related ECD moves on the adjacent bank of the fusiform gyrus. Therefore, hue-response and luminance-response would be spatially segregated.

Although ECDs representing twelve colors are all localized in V4α, the shapes of them are different from each other. The pair of refined orbits for similar color has a similar shape with each other. Figure 8 shows orbits of ECDs within V4α for each color. Orbits are colored by the corresponding color to the respective stimuli (Note: Those are lying within quite a small volume 1 [cm^3]). The shape of each orbit is similar to that of the similar color. Therefore, the topology of hue space would be conserved in a space of the deformation of the orbital shapes. (Colored figures can be seen in the FORMA's WEB pages.)

6. Conclusion

Generally, the mappings of the primary brain function to the cortical area are topological. For example, there exist "retinotopy", "somatotopy", "tonotopy", and etc. Though we know color perception is mapped into V4, we do not know how the topology of the color perception is, however, mapped within V4. Every color stimulus activates V4α whereas each color has a characteristic orbit within V4 that is responding to the color stimulus. This mapping appears to conserve the topological relation in terms of the deformational space of the ECD orbits. In the other words, chromatic topology is conserved in the coarse-grained current-dipole orbit. Our results suggest that the neural coding of a color is represented by a spatiotemporal activity in V4α (spatiotemporal representation). Our nonparametric gICA algorithm successfully separates the raw data into the independent components that are considered to be localized activities in the brain. This separation provides us a simplification that makes it possible that we can transfer the inverse problem into a simple estimation problem of single current dipole. Consequently, we have obtained quite a fine spatial resolution in the order of 1 [mm] in MEG measurements.

This research has been partially performed through Academic Frontier Program "Neurocognitive Research on Cognition, Language and Behavior by Non-Invasive Brain-Function Measuring Technology" and Special Coordination Fund for the promotion "Neuroinformatics Research in Vision" of Ministry of Education, Culture, Sports, Science and Technology, of the Japanese Government.

REFERENCES

AMARI, S. (1998) Natural gradient works efficiently in learning, *Neural Computation*, **10**(2), 251–276.

BARTELS, A. and ZEKI, S. (2000) The architecture of the color centre in the human visual brain: new results and a review, *European Journal of Neuroscience*, **12**, 172–193.

HADJIKHANI, N., LIU, A. K., DALE, A. M., CAVANAGH, P. and TOOTELL, R. B. H. (1998) Retinotopy and color sensitivity in human visual cortical area V8, *Nature Neurosci.*, **1**, 235–241.

KELLY, D. H. and VAN NORREN, D. (1977) Two-band model of heterochromatic flicker, *J. Opt. Soc. Am.*, **67**(8), 1081–1091.

LIVINGSTONE, M. and HUBEL, D. H. (1988) Segregation of form, color, movement, and depth: anatomy, physiology, and perception, *Science*, **240**, 740–749.

MCKEEFRY, D. J. and ZEKI, S. (1997) The position and topography of the human colour centre as revealed by functional magnetic resonance imaging, *Brain*, **120**, 2229–2242.